KinomeMETA: meta-learning enhanced kinome-wide polypharmacology profiling

Qun Ren[3,1#], Ning Qu[1,2#], Jingjing Sun[1,2], Jin Liu[4,1], Lin Ni[1,2], Xiaochu Tong[1,2], Zimei Zhang[1], Xiangtai Kong[1,2], Yiming Wen[5,1,2], Yitian Wang[1,2], Dingyan Wang[6], Xiaomin Luo[1,2], Mingyue Zheng[1,2,3,5*], Xutong Li[1,2*]

[1] Drug Discovery and Design Center, State Key Laboratory of Drug Research, Shanghai Institute of Materia Medica, Chinese Academy of Sciences, 555 Zuchongzhi Road, Shanghai 201203, China

[2] University of Chinese Academy of Sciences, No.19A Yuquan Road, Beijing 100049, China

[3] Nanjing University of Chinese Medicine, 138 Xianlin Road, Nanjing 210023, China

[4] College of Pharmaceutical Sciences, Zhejiang University, Hangzhou 310058, China

[5] School of Pharmaceutical Science and Technology, Hangzhou Institute for Advanced Study, UCAS, Hangzhou 330106, China

[6] Lingang Laboratory, Shanghai 200031, China

[#] Qun Ren and Ning Qu have contributed equally to this work

[*] Correspondence: myzheng@simm.ac.cn; lixutong@simm.ac.cn

Abstract

Kinase inhibitors are crucial in cancer treatment, but drug resistance and side effects hinder the development of effective drugs. To address these challenges, it is essential to analyze the polypharmacology of kinase inhibitor and identify compound with high selectivity profile. This study presents KinomeMETA, a framework for profiling the activity of small molecule kinase inhibitors across a panel of 661 kinases. By training a meta-learner based on a graph neural network and fine-tuning it to create kinase-specific learners, KinomeMETA outperforms benchmark multi-task models and other kinase profiling models. It provides higher accuracy for understudied kinases with limited known data and broader coverage of kinase types, including important mutant kinases. Case studies on the discovery of new scaffold inhibitors for PKMYT1 and selective inhibitors for drug-resistant mutants of FGFRs demonstrate the role of KinomeMETA in virtual screening and kinome-wide activity profiling. Overall, KinomeMETA

has the potential to accelerate kinase drug discovery by more effectively exploring the kinase polypharmacology landscape.

Introduction

Protein kinase-mediated cellular signaling pathways are responsible for a range of physiological and pathological processes. Kinase-targeted inhibitors have emerged as a promising therapeutic approach and have been applied clinically for a wide range of diseases, including cancer and inflammation[1, 2]. However, due to the structural similarity of kinases, many kinase inhibitors modulate multiple target proteins, resulting in either therapeutic effects or unwanted side effects. Single-target kinase inhibitors are preferred as have fewer off-target interactions and lower side-effect risks, making them clinically safer[3]. However, many severe diseases require modulation of multiple targets or overcoming therapeutic resistance, leading to the development of multi-target kinase inhibitor. Such inhibitors have the potential to be more effective than individual inhibition processes, which are frequently bypassed by alternative compensatory biological routes[4, 5].

Kinase inhibitors which can target multiple signaling pathways with minimal risks associated with polypharmacy are crucial for developing highly effective targeted therapies. To design and optimize kinase-targeted drugs rationally, it is essential to gain insights into the selectivity or promiscuity of inhibitors. Kinome-wide activity profiling can provide multidimensional structure–activity relationships simultaneously against hundreds of kinases, but experimental screening for a broad spectrum of kinases remains time-consuming, technically challenging, and costly[5, 6]. Moreover, this type of profiling is usually carried out during the later stages of drug discovery, making it challenging to offer guidance for molecular design. Recent advances in deep learning technology have made in-silico screening assays more reliable, allowing investigators to annotate compounds with the kinase spectrum more rapidly and cost-effectively in the early stages of drug discovery. Various models have been proposed to predict the polypharmacological effects of small molecular kinase inhibitors, such as naive Bayes (NB)[7], Random forest (RF)[8], Support vector machine (SVM)[7, 9, 10, 11] and Deep neural network (DNN)[12, 13]. Merget et al. used single-task (ST) random forest to create activity prediction models for more than 280 kinases. They showed that models with a high number of active compounds (more than 1000) typically have auROC values above 0.8[8]. In our prior work we developed a multi-task (MT) DNN model based on the

molecular ECFPs to predict the inhibitory effects of small molecules against 391 kinases. The MT-DNN model showed superior performance over ST machine learning (ML) models with an average auROC of 0.90, especially for kinases with limited activity data. The generalization ability of MT-DNN demonstrated that multi-task transfer learning is an effective strategy for the prediction of a large panel of kinases[14]. Recently, Bao et al. applied graph neural networks (GNNs) to MT learning to predict the inhibition profiles for small molecules against 204 kinases. GNNs can produce task-specific representation for molecules and has been proved to have better performances than models based on pre-defined descriptors[15]. In addition to ligand-based strategies, multidimensional relationships can also be constructed from the perspective of heterogeneous networks that describe the compound-protein interactions. IDDkin applied graph convolution networks (GCNs) to diffuse the information of heterogeneous networks to enhance the prediction of kinase inhibitors[16]. However, network-based methods have limitations in the case of large graphs, making it hard to diffuse information for large-scaled datasets of compound-kinase pairs. Therefore, only around 1000 molecules were used for building the network of IDDkin.

Developing virtual profiling methodologies for kinases presents a challenge due to insufficient data for understudied kinases. This limitation is a significant bottleneck for accurately predicting a broader spectrum of kinases, particularly “dark” or mutant kinases, where the number of known active compounds is insufficient for building accurate models. Additionally, existing models for predicting kinases are often not extensible, making it difficult to generalize to new kinases that have not been included in training (unseen tasks). Even if additional data are obtained from new literature or wet-lab experiments, traditional models struggle to incorporate this new data and extend the predictable kinase spectrum.

Meta-learning is a promising algorithm that can address the challenge of low-data, which leverages previous knowledge acquired from data to solve novel tasks quickly and efficiently. Meta-learning has been adopted in some fields of drug discovery, such as molecule optimization[17], drug response prediction[18], chemical-protein interactions prediction[19], T-cell receptor-antigen binding recognition[20], etc. The advantages are as follows: the ability to learn from a handful of

examples, learning or adapting to novel tasks quickly, and the capability to build more generalizable systems[21]. Therefore, meta-learning has the potential to become a new paradigm for the future drug discovery, which demands a closed-loop automated procedure that synergies between the components of the conventional discovery procedures and extensible AI methods[22].

This study presents KinomeMETA, a general framework for profiling the activity of small molecule kinase inhibitors across a panel of 661 kinases. One of the key challenges in virtual profiling methodologies for kinases is the limited availability of data, particularly for some mutant forms and understudied kinases. To address this challenge, KinomeMETA utilizes a modified meta-learning strategy integrated with a graph neural network. This strategy enables KinomeMETA to effectively learn from limited data and enhance its predictive capabilities, thus expanding the coverage of kinome-profiling. Additionally, the framework incorporates fast fine-tuning that enables it to generalize to unseen kinases with high accuracy, overcoming the limitations of previous machine learning models that were restricted to specific kinases within their modeling domains (Fig. 1). We assess the performance of KinomeMETA from three different perspectives, corresponding to different application scenarios including kinome-wide activity profiling, mutant kinase selectivity prediction, and rapid adaptation to previously unseen kinases. Moreover, we apply KinomeMETA in these practical scenarios, such as the discovery of new scaffold inhibitors for PKMYT1 and retrospective analysis of selective inhibitors for drug-resistant mutants of FGFRs. By integrating it into the iterative predict-experiment cycles, we show that KinomeMEAT can aid in the rational design of kinase inhibitors with a more favorable selectivity profile. This paves the way for the development of more effective targeted therapies.

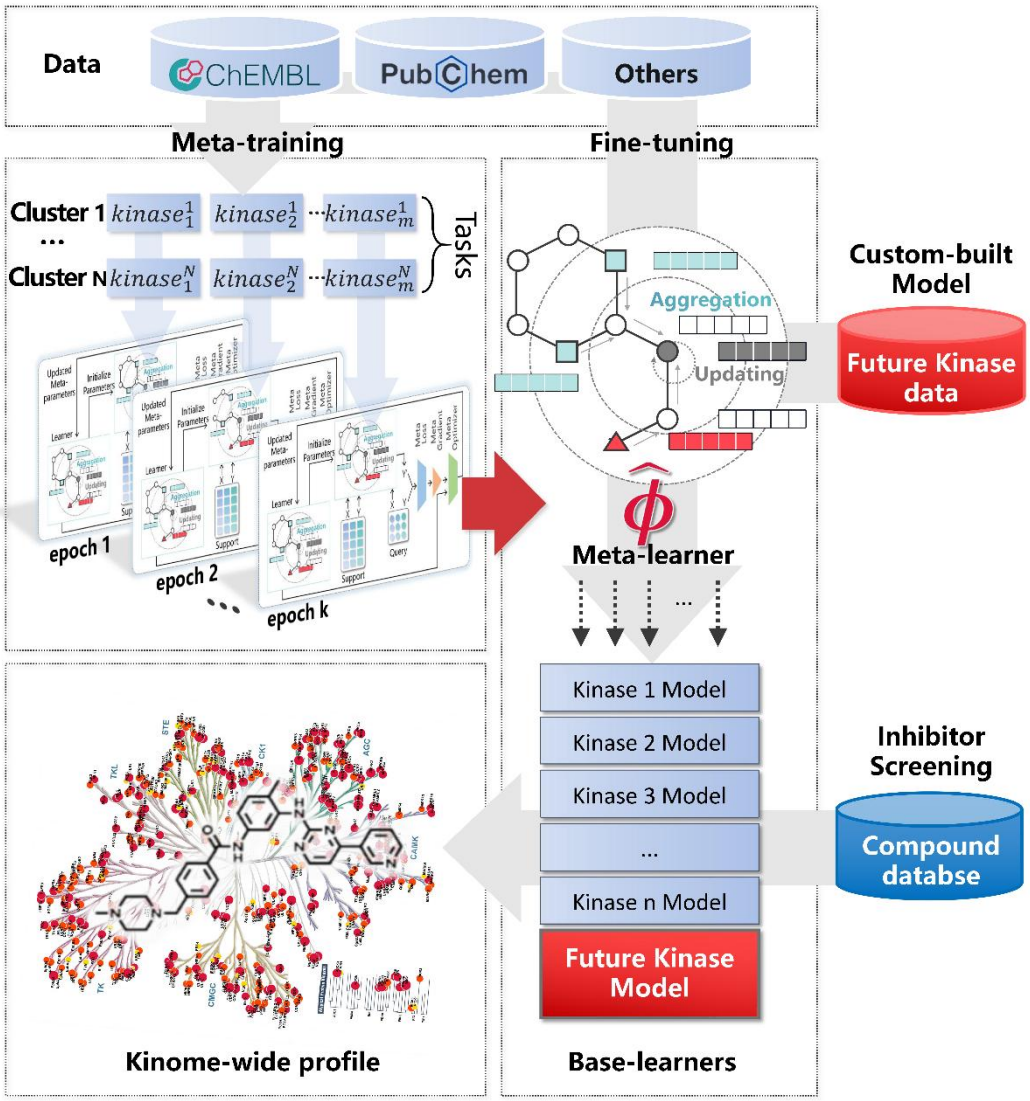

111

112 **Fig. 1 | The overall architecture of KinomeMETA.**

113

114

115 ## Results

116 ### Processing Kinase Inhibitor Data

117 The structure and activity data of kinase-compound pairs were collected and integrated from
118 open-source databases, ChEMBL[23], PubChem[24] and DKKB[25] (Dark Kinase Knowledgebase)
119 Briefly, those kinase-compound pairs passing the following filters were retained: (i) the assay type
120 was binding, (ii) the bioactivity type was IC_{50}, K_i, EC_{50}, K_d or %Inh and (iii) the target is single
121 protein kinase whose confidence score is 9 in ChEMBL. For building classification model,

bioactivity data were converted to two classes: positive (pK_i/pK_d/pIC_{50}/pEC_{50} ≥ 6 or %Inh ≥ 80%) and negative (pK_i/pK_d/pIC_{50}/pEC_{50} < 6 or %Inh < 80%). Only kinases with positive compounds were kept. Specifically, the final datasets encompass over 612,000 manually curated bioactivity datapoints, spanning over more than 160,000 distinct compounds and 661 kinases, including 118 mutants. The specific data statistics are shown in Fig. 2. There are 543 wild-type kinases that mainly belong to Homo sapiens, Mus musculus and Rattus norvegicus (Fig. 2c), along with 118 mutations involving 44 different kinases, mostly human tyrosine kinases (TK) and tyrosine kinase-like (TKL) kinases (Fig. 2d). Furthermore, as meta-learning reduces the demand for training data, a large number of kinase domains with data records less than 50 were retained to build a broader task panel, including kinases that have not been fully studied and some rare mutation types (Fig. 2a and 2b).

In addition, we have built a credible set of negative samples to reduce false positive predictions caused by the imbalanced distribution of samples. In real-world virtual screening scenarios, negative results often greatly outnumber positive results, but the experimentally-validated negative samples are often insufficient. Here, three property-matched decoys[26] have been sampled for each positive data from BindingDB database, resulting in a negative-positive ratio of approximately 1:5 in the final datasets. The distribution of molecular weight and logP of decoys is relatively consistent with that of the original samples (see Supplementary Fig. 1). This approach encourages the model to learn an information-rich representation of molecules rather than biases in their properties, thus improving its prediction accuracy.

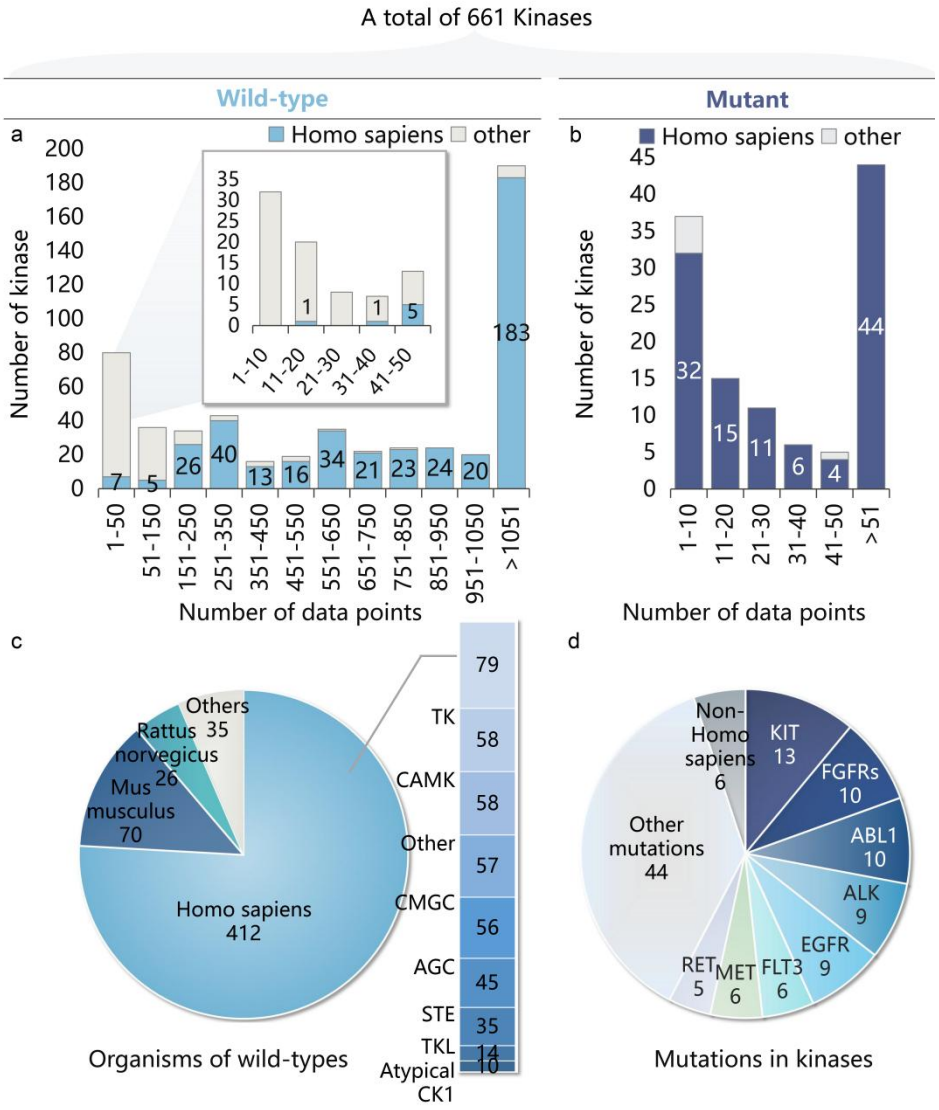

Fig. 2 | Statistics of the dataset. a, Statistics of wild-type kinase data: Histogram illustrates the distribution of tasks across different ranges of data sizes. Each task represents a class of kinase and data points correspond to the inhibitors of the kinase. The light blue area within each bar represents the number of Homo sapiens kinases, while the gray area represents kinases from other organisms. **b,** Statistics of mutant kinase data. The dark blue area within each bar represents the number of Homo sapiens kinases, while the gray area represents kinases from other organisms. **c,** Distribution of organisms and subfamilies of wild-type kinases. **d,** Distribution of subfamilies of mutant kinases.

The implementation of KinomeMETA

KinomeMETA is a general framework designed to assess the probabilities of a molecule inhibiting a panel of kinases. The framework integrates a model-agnostic meta-learning algorithm, Reptile[27], with Attentive-FP[28], a graph attention neural network-based molecular representation model. Kinases are considered to be broadly related tasks, many of which are not thoroughly studied and therefore qualify as few-shot tasks. The meta-learning algorithm generates a well-generalized meta-learner by training it on a distribution of various learning tasks that are intrinsically related. As a result, the meta-learner can transfer new tasks with just a few training samples, making it suitable for few-shot learning.

To implement KinomeMETA, the collected kinases were divided into training tasks T^{train}, validation tasks T^{valid} and test tasks T^{test} at task level. T^{train} were used to train a meta-learner with the optimal initialization parameters, while both T^{valid} and T^{test} were used to build kinase-specific base-learners for evaluating the generalization of the meta-learner in fine-tuning scenarios. Specifically, T^{valid} was used for optimizing the meta-learner, whereas T^{test} was used for the comparisons with other methods. At the instance level, 20% of the compounds in every task were segregated for testing the performance of the kinase-specific base-learners. In the training tasks, the remaining compounds were further randomly divided into a support set and query set at a ratio of 4:1, similar to a normal meta-learning process (Fig. 3a).

During the meta-training phase, the meta-learner performs multiple gradient descents within the task by utilizing the support set. This process generates a model that updates its parameters based on the prediction errors made on the query set, as shown in Fig. 3b. In the fine-tuning phase, the meta-learner undergoes additional gradient steps on the support set of N test tasks, creating N task-specific base-learners that can effectively classify examples in the query set for each of the N test tasks, as shown in Fig. 3c. To build KinomeMETA for the specific case of N-way K-shot few-shot classification problems, we selected the strategy of 2-way 3-shot classification. This means that for each of the two classes of compounds (N = 2), namely positive and negative, we sampled three compounds (K = 3, determined through hyperparameter searching as shown in Supplementary Fig. 3 and Supplementary Table 1) for the selected kinase tasks.

In fact, we do not need to train the meta-model with a fixed partition ratio of tasks to establish a generalizable meta-learner, but only with a few representative kinase tasks. Transferring knowledge among tasks with heterogeneous attribute spaces, such as kinases, is

challenging in general meta-learning framework. To address this challenge, we have modified the meta-training strategy by training the meta-learner hierarchically in a task cluster-wise manner, based on the hierarchical cluster of the task representations for 661 kinases (see Fig. 3d for details, as well as the Method sections and Supplementary materials). We sampled kinases from every cluster as equally as possible and progressively added them into the meta-learner as training tasks. After training on 113 kinases, we obtained a meta-learner with the best generalization, with an average MCC of 0.73 on validation tasks (Supplementary Fig. 2c). By progressively training the meta-learner in a cluster-wise manner, we can balance the knowledge learned across heterogeneous kinase tasks, preventing the meta-model from being dominated by closed tasks in the majority cluster and improving its generalization. Supplementary Fig. 2c compared the cluster-wise training strategy with the baselines by adding random tasks iteratively or by adding all tasks in the first iteration.

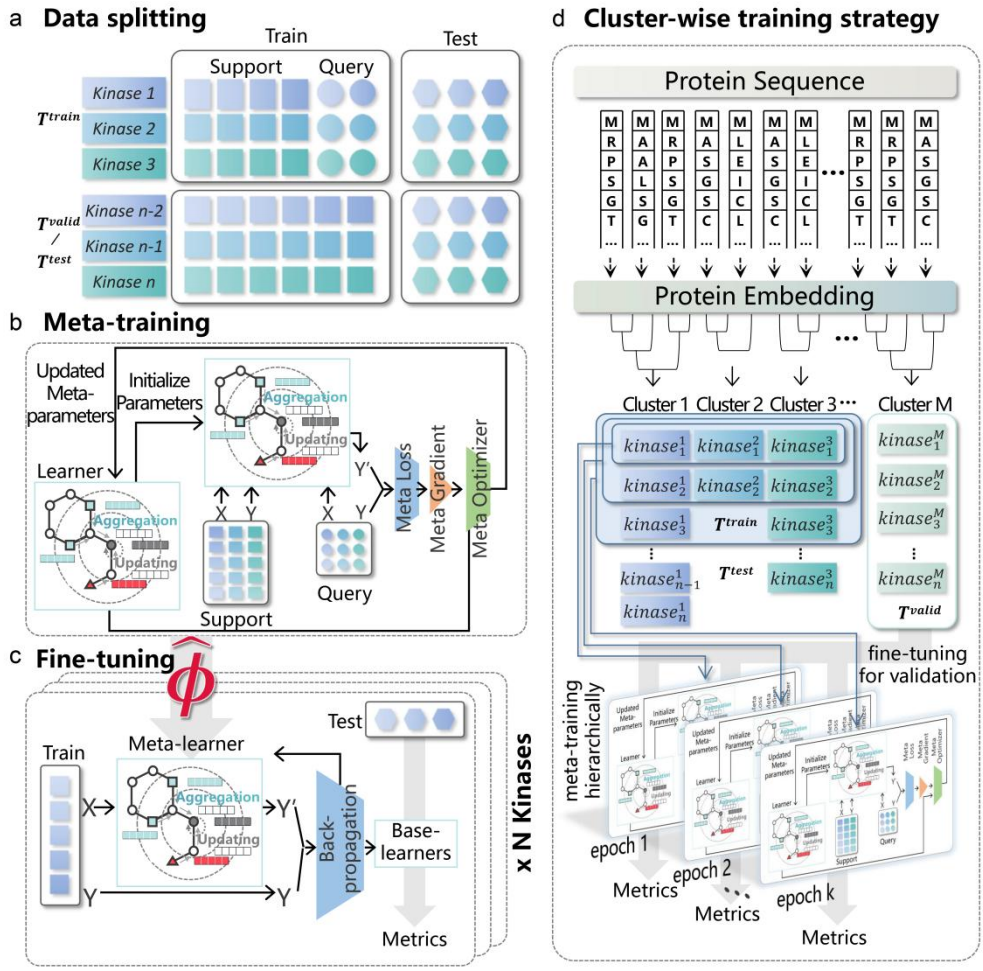

Fig. 3 | Data Splitting Strategy and Training Process. a, Data Splitting Strategy. **b,** The meta-training phase. **c,** The fine-tuning phase. **d,** Cluster-wise training strategy.

KinomeMETA demonstrates high performance for kinase profiling

During the meta-training phase, the meta-learner was established in a task cluster-wise manner, involving 113 kinases. In the subsequently fine-tuning phase, the meta-learner was optimized for unseen tasks originating from a diverse attribute space. To enable comprehensive polypharmacology profiling across the kinome, a panel of fine-tuned models encompassing 661 kinases including training, validation and test tasks needed to be constructed and assessed. Our objective was to evaluate the performance of KinomeMETA from three different perspectives, corresponding to various application scenarios. First, we evaluated the overall performance on kinome-wide tasks. This involved constructing kinase-specific base-learners for all kinases not included in the meta-training set (T^{test}), and assessing the model's generalization capabilities. Additionally, we built base-learners for the 113 tasks in T^{train}, which formed the foundation of the kinome-wide virtual screening panel essential for evaluating inhibitor selectivity. Second, we assessed KinomeMETA's performance on tasks involving mutated kinases, as kinase mutations play a critical role in human diseases, particularly in cancer, and are of significant interest. Lastly, we evaluated KinomeMETA's performance on few-shot kinase tasks that were not incorporated during the model's training phase. Evaluating unseen few-shot tasks was given priority to demonstrate the meta-learning's ability to construct more generalized systems. Moreover, few-shot tasks corresponded to kinases with limited characterization, making them particularly worth exploring.

We implemented a baseline method that uses a multi-task transfer learning approach based on Graph Neural Networks (GNN). The multi-task GNN model (MTGNN) is based on our previous work[14], which was initially pre-trained on T^{train} and subsequently fine-tuned on each task in T^{test}, following the similar procedure as KinomeMETA. Further implementation details can be found in the Supplementary materials and Supplementary Fig. 7.

Overall performance on kinome-wide tasks. KinomeMETA outperforms MTGNN on both meta-training tasks T^{train} and unseen tasks T^{test}. It adapts well to tasks within the training field (Fig. 4a) while maintaining a high level of generalization to unseen kinases. Fig. 4b showed that

most kinase-specific learners built from KinomeMETA have MCCs above 0.6 (452 out of 517 test tasks). This suggests that KinomeMETA can provide accurate predictions for kinome-wide activity profiles. Specifically, for 412 predictable wild-type human kinases, MCCs of 189 kinases are higher than 0.8, while only 12 of them have MCCs less than 0.4 (Fig. 4c and Supplementary Table 5 provides details on each task). These results confirmed that KinomeMETA has overcome the limitations of previous models that could only predict a small range of targets, achieving the goal of large-scale kinase prediction and selectivity analysis.

Performance on mutations tasks. Generalizing to mutants of kinases is a challenging task. This challenge stems not only from insufficient data but also from inherent conflicts resulting from data distribution differences among tasks. In other words, molecules for wild-type kinases and corresponding mutant tasks may have some opposing labels due to drug resistance caused by mutations. In transfer learning, these distribution differences can lead to negative transfer, especially when model parameters are extensively shared across all tasks, such as in MTGNN[29]. To examine whether KinomeMETA can adapt to the different distribution between wild-type kinases and their mutant forms, we compared it with MTGNN and another baseline model called "SameAsWild". This baseline represents an overfitted model that can only learn the label distribution from wild-type kinases and transfer this "naïve knowledge" to their mutant forms.

When compared to MTGNN, KinomeMETA demonstrates significantly superior performance on mutation tasks (Fig. 4d). Further evaluation for each kinase with at least four mutation types reveals robust performance of KinomeMETA for the majority of mutations. As shown in Fig. 4e, the data points mostly concentrated in the second and fourth quadrants, indicating higher MCC values of KinomeMETA. In contrast, MTGNN shows MCCs of 0 for many tasks. Comparing with "SameAsWild," KinomeMETA also exhibits substantial superiority (Fig. 4d). This is true even when modeling data is scarce, as exemplified by KIT-D820Y, KIT-K642E, and KIT-Y823D shown in Fig. 4f (refer to Supplementary Fig. 4 for labels of samples in KIT and its mutant forms; Supplementary Fig. 5 displays the heatmaps for other kinases' mutant forms). In addition, MTGNN demonstrates moderate performance similar to "SameAsWild" (Fig. 4d) and even performs worse than "SameAsWild" in certain mutant tasks due to negative transfer. These results demonstrate that KinomeMETA can identify the drug resistance of wild-type kinase's active compounds to their mutant forms, rather than simply overfitting to the training data. This ability

can be attributed to the advantage of the meta-learning approach employed by KinomeMETA, which mitigates overfitting through two different time scales of learning: slow learning for common features of molecular interactions with kinases during meta-training phase, and fast learning for task-specific aspects of kinase inhibition in the fine-tuning phase. This combination allows meta-learning to develop an understanding of a wide range of kinase tasks from more stable parts, while also enabling faster adaptation for changes with less data[30]. This ability is crucial for the successful screening of inhibitors targeting drug-resistant kinase mutants.

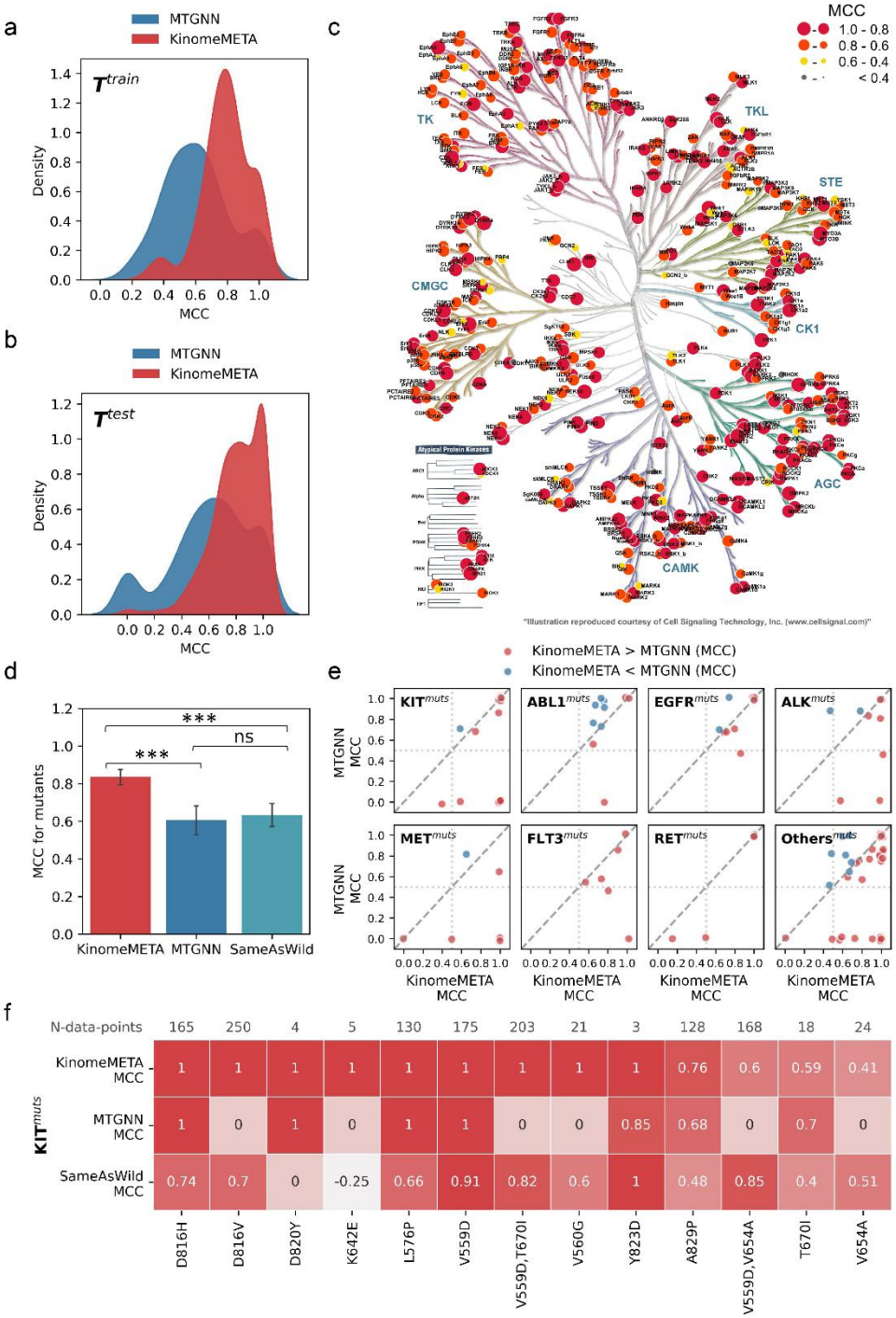

Fig. 4 | **The performance of KinomeMETA on overall tasks and mutations tasks. a,** The MCC-based performance comparison between KinomeMETA and MTGNN on the training tasks. **b,** The MCC-based performance comparison between KinomeMETA and MTGNN on test tasks. **c,** The phylogenetic tree of 412 predictable wild-type human kinases, with each point representing the MCC of a specific kinase. **d,** The MCC-based performance comparison between KinomeMETA, MTGNN and "SameAsWild" on human kinase mutation tasks. The statistical

analyses were performed by one-tailed Wilcoxon Signed-Rank test. (*) $0.01 < p \leqslant 0.05$; (**) $0.001 < p \leqslant 0.01$; (***) $p \leqslant 0.001$. **e,** The performance of KinomeMETA and MTGNN for kinases with over 4 mutation types (KIT^{muts}, $ABL1^{muts}$, $EGFR^{muts}$, ALK^{muts}, MET^{muts}, $FLT3^{muts}$, and RET^{muts}), as well as for kinases with less than 4 mutation types ($Others^{muts}$). The scatter plot visualizes the relationship between KinomeMETA and MTGNN MCC values for different mutants of corresponding wild-type kinases. Each point on the plot represents a mutant form, with red points indicating a higher MCC for KinomeMETA and blue points representing a higher MCC for MTGNN. **f,** The performance of KinomeMETA for KIT mutants, comparing it to MTGNN and the "SameAsWild" prediction, all measured by MCC.

Performance on few-shot learning tasks. When addressing few-shot tasks through meta-learning, the size of the available data affects the fine-tuning performance. While having more available data should improve task-specific base-learners, training understudied kinase tasks with a very large amount of data is impractical. KinomeMETA aims to reduce data requirements in such cases. We conducted a statistical analysis of model performance across kinases with varying data sizes and found that KinomeMETA is effective for kinases with less than 50 active samples (as shown in Fig. 5a). In fact, KinomeMETA significantly outperformed MTGNN for all ranges of data sizes (Fig. 5b).

We designed a data-adding experiment to demonstrate the usage of KinomeMETA in a low-data scenario for drug discovery. Specifically, we selected EGFR, a kinase with a large dataset of 6250 active compounds in T^{test} to simulate the low-data scenario. We trained EGFR-specific base-learners with increasing data size to determine when we could achieve satisfactory performance. This process is referred to as a "data-adding experiment". We evaluated the performances of KinomeMETA, MTGNN, and a "random prediction" baseline model on 20% of the compounds, which were randomly and consistently split. The results are shown in Fig. 5c measured by MCC and Supplementary Fig. 6 measured by auROC. Comparing with the "random prediction" model can verify the effectiveness of the trained model. To do this, we randomly assigned active/inactive labels to test compounds and calculate the metrics with true labels. With one-shot learning setting, i.e., training with one active and one inactive compound, KinomeMETA's EFGR model achieved an MCC of 0.11 and an auROC of 0.62, while the

306 “random prediction” model achieved an MCC of 0 and an auROC of 0.5. These findings
307 demonstrated that KinomeMETA can effectively learn from a very small amount of data.
308 Furthermore, KinomeMETA was able to be optimized more quickly than MTGNN when the data
309 size was increased by adding an active and an inactive data point each time. The performance gap
310 between KinomeMETA and MTGNN increased as well. Within only 20-shot learning,
311 KinomeMETA achieved a strong performance (MCC = 0.68, auROC = 0.91), which was close to
312 the performance achieved when training with all 4999 active compounds in the training set (MCC
313 = 0.72, auROC = 0.92). In contrast, MTGNN had slower performance growth and earlier
314 convergence, resulting in significantly lower performance metrics compared to KinomeMETA.
315 The size of the training data plays a crucial role in determining the predictive power of a
316 task-specific base-learner. However, KinomeMETA demonstrated impressive performance on
317 different fine-tuning shot numbers, highlighting its practical value in low-data scenarios for
318 understudied kinases. Additionally, modeling with few-shot kinases offers an added benefit of
319 quickly training new models for previously unseen kinases. With as few as 10 samples,
320 KinomeMETA can be used to construct a model with decent performance for a new task. This
321 means that KinomeMETA can be continuously extended to effectively address the problem of
322 previous machine learning models that could only predict specific kinases within their modeling
323 domain.

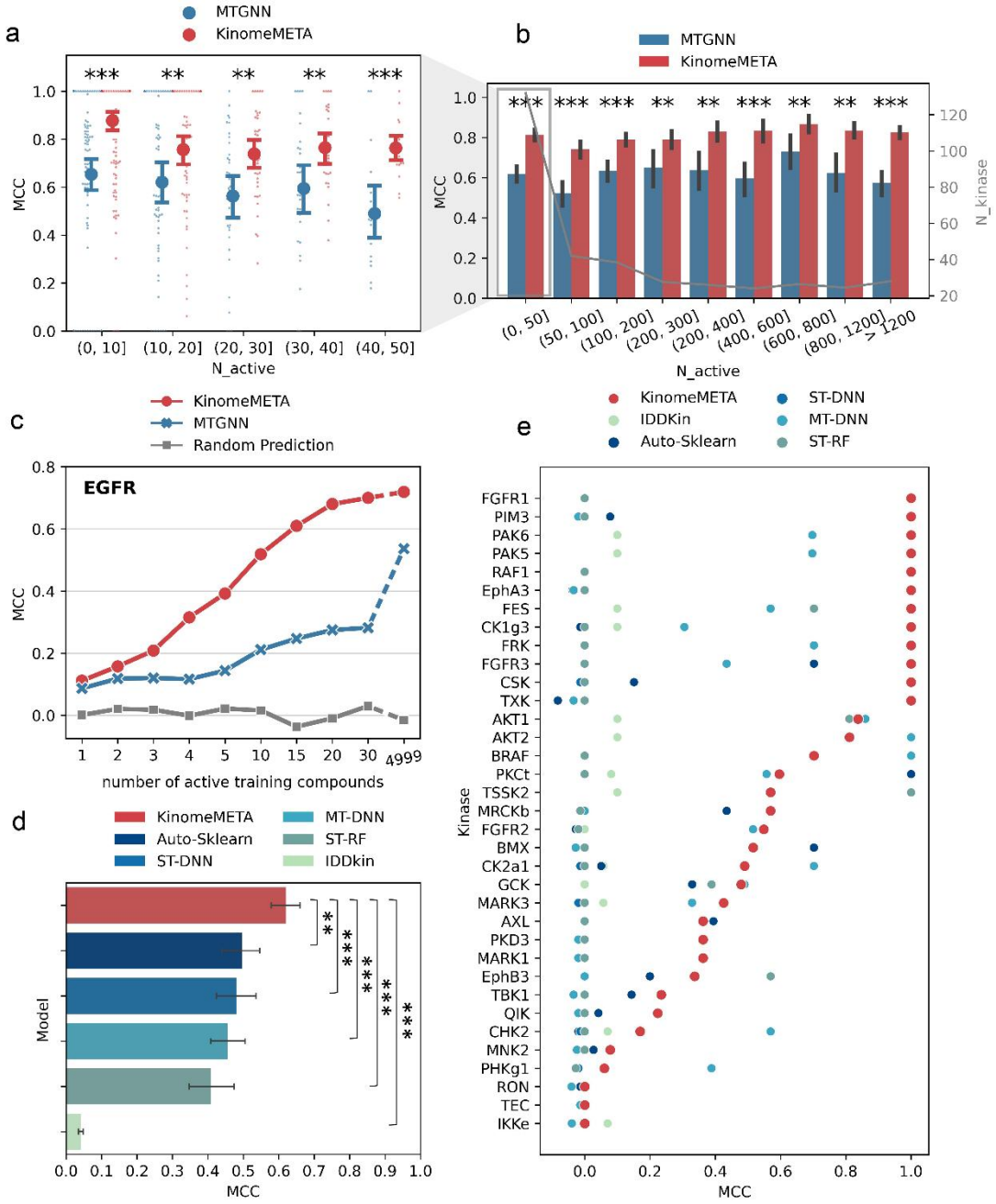

Fig. 5 | KinomeMeta's performance on few-shot learning tasks and comparison with previous models. a, Performance comparison between KinomeMETA and MTGNN on few-shot learning setting, where the range of training active compounds is from 1 to 50. For each range, small scatters represent the Matthews correlation coefficient (MCC) of each task in the corresponding range, while the large scatters with error bars represent the average and standard deviation of them. **b,** Overall performances comparison between KinomeMETA and MTGNN using a bar plot. Each bar indicates the average MCC of tasks within the underlying range, and its error bar indicates standard deviation of them. KinomeMETA is colored in red and MTGNN in

blue. **c,** Performance comparison between KinomeMETA and MTGNN in the data-adding experiment, in terms of MCC. **d,** Comparing KinomeMETA's performance with RF, MT-DNN, IDDkin, ST-DNN and Auto-Sklearn based on the dataset of IDDkin. Bar plots of model performance on MCC. A bar indicates the average MCC of all modelling kinase tasks, and its error bar indicates standard deviation of them. **e,** Comparing KinomeMETA's performance with RF, MT-DNN, IDDkin, ST-DNN and Auto-Sklearn based on the dataset of IDDkin on few-shot kinase tasks (< 10 active data points) measured by MCC. All Statistical analyses were performed by one-tailed Student's t-test. (*) $0.01 < p \leqslant 0.05$; (**) $0.001 < p \leqslant 0.01$; (***) $p \leqslant 0.001$.

KinomeMETA outperforms previous kinase profiling models

We conducted a comparative analysis of KinomeMETA and several machine learning methods for kinase profiling, including RF[8], multi-task DNN[14] (MT-DNN) and network-based IDDkin[16]. Additionally, we evaluated two widely used general target prediction methods: single-task DNN (ST-DNN) and Auto-Sklearn[31]. Since IDDkin is not suitable for large graphs due to the use of the GCN, we used the modelling dataset reported in IDDkin to train the meta-learner of KinomeMETA and fine-tuned it on these kinases. The remaining methods were also trained using the same dataset as IDDkin. The implement of each method can be found in the Supplementary materials, and the parameter settings for each model are provided in Supplementary Table 2.

The results show that KinomeMETA outperformed all other methods significantly (Fig. 5d and Supplementary Table 3). Fig. 5e illustrates the kinase-specific performance of each algorithm on 35 few-shot learning tasks that have less than 10 positive training samples. KinomeMETA exhibited superior performance on 22 tasks, with MCC over 0.4 for 23 tasks, demonstrating its robustness. Single-task algorithms exhibit quite unstable performances on these tasks. Auto-Sklearn achieved MCC values higher than 0.4 on four tasks, while ST-DNN failed to achieve values higher than 0.4 on any task. In contrast, the performance of multi-task algorithms, such as MT-DNN, was relatively stable on few-shot kinases, with 11 kinases' MCC above 0.4, as previously reported[14]. However, the average MCC of MT-DNN is moderate, possibly due to negative transfer for some tasks caused by the hard parameter sharing mechanism. IDDkin, the

network model, performed only slightly better than random prediction when measured by MCC. Although IDDkin has previously reported high auROC values, it had very low F1-scores, which can be attributed to treating all unknown kinase-compound pairs as negative samples during training, resulting in biased prediction. In conclusion, KinomeMETA consistently outperformed other models in most kinases, particularly in those with less known data, regardless of whether it is a single-task, multi-task, or network algorithm. The robustness of KinomeMETA further supports its ability to enhance kinome-wide virtual profiling.

KinomeMETA-aided discovery of kinase inhibitors

Discovery new scaffold inhibitors for PKMYT1. Kinases are key targets for therapeutic development efforts, but the biological function of nearly one-third of kinases is largely unknown. The Dark Kinase Knowledgebase (DKKB; https://darkkinome.org) is specifically focused on developing a better understanding of the approximately 160 understudied kinases whose function in human biology is poorly understood[25]. Among them, the membrane-associated tyrosine- and threonine-specific cdc2-inhibitory kinase (PKMYT1) is of particular interest and has been selected in the early stages of this project. PKMYT1 preferentially phosphorylates and inactivates cyclin-dependent kinase 1 (CDK1), and is a compelling therapeutic target for the treatment of certain types of DNA damage response cancers due to its established synthetic lethal relationship with CCNE1 amplification[32].

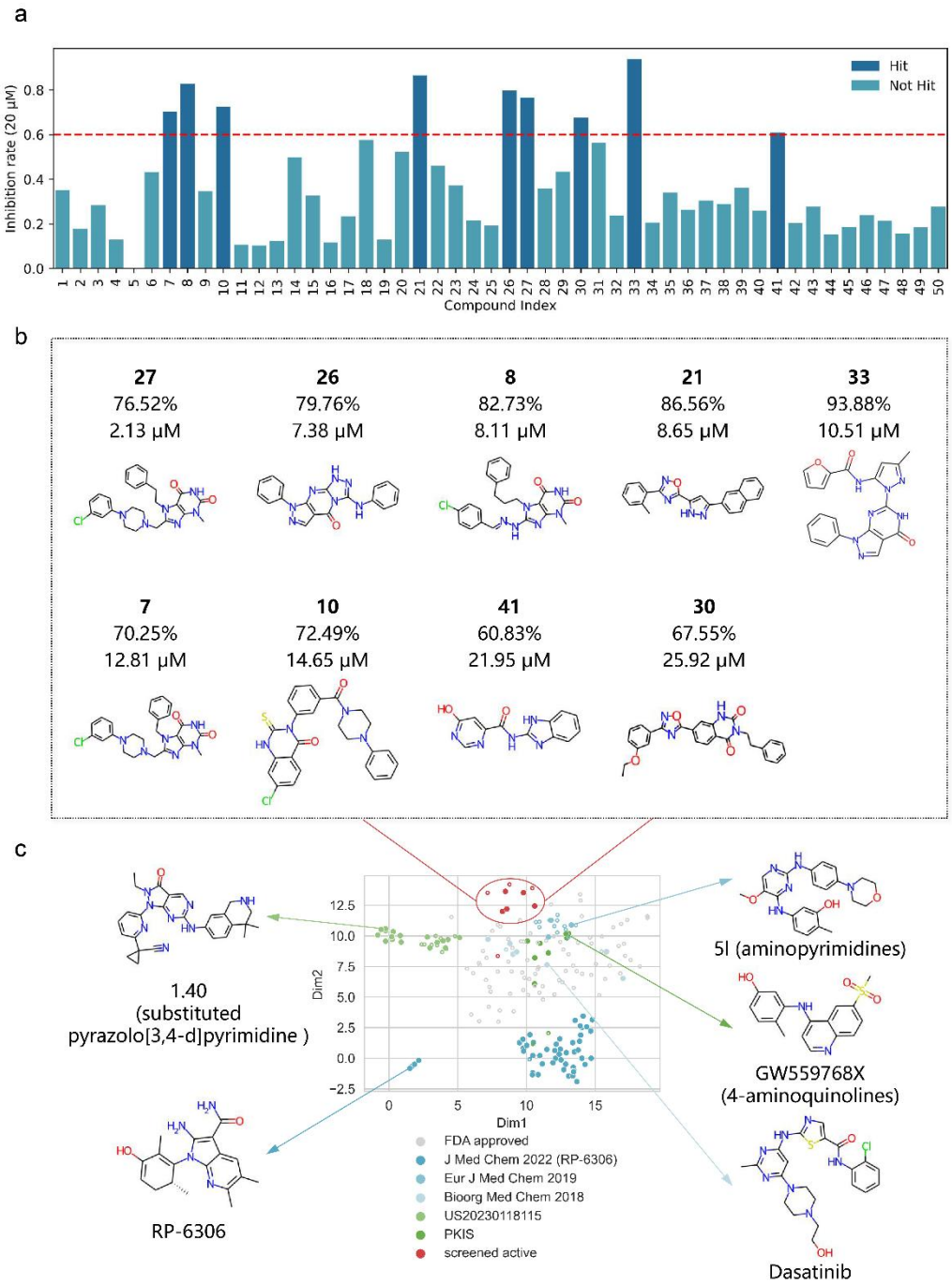

383

384 **Fig. 6 | The screening results of PKMYT1. a,** The inhibition rates for 50 screened compounds at
385 an inhibitor concentration of 20 μM. **b,** The inhibition rates, IC_{50} and structures for 9 compounds
386 with inhibition rate >60%. **c,** Uniform manifold approximation and projection (UMAP) and
387 representative chemical structures for FDA approved kinase-targeted drugs (gray scatters), new
388 identified PKMYT1 inhibitors (red scatters), previously reported PKMYT1 inhibitors (a variety of
389 blue and green scatters).

390

PKMYT1 is a highly selective kinase that is difficult to inhibit compared to other kinases. According to a comprehensive analysis of kinase inhibitor selectivity by Davis et al.[33] only 4.17% of the tested compounds inhibit PKMYT1, including the multi-targeted tyrosine kinase inhibitors dasatinib (Fig. 6c), bosutinib, and some pyridopyrimidine derivatives[34]. Only 2% of all the tested kinases have such low propensity for compound binding. Platzer et al.[35] tested 800 compounds from kinase inhibitor libraries PKIS I and II and identified only 10 PKMYT1 inhibitors with IC_{50} values in the nanomolar and micromolar range (e.g., GW559768X in Fig. 6c). They subsequently designed a set of diaminopyrimidine derivatives, which are active in the sub-micromolar range (e.g. compound 5l in Fig. 6c)[36]. A patent (US11332473B2)[37] claimed a set of substituted pyrazolo[3,4-d]pyrimidines as Wee1 inhibitors, in which compound "1.40" is active against PKMYT1 with an IC_{50} of 0.121 μM. In 2022, Szychowski et al.[38] reported the discovery of the first potent, selective, and orally bioavailable PKMYT1 inhibitor, RP-6306. This inhibitor shows an IC_{50} of 0.002 μM, and high selectivity observed over the highly homologous enzyme Wee1.

Currently, PKMYT1 inhibitors are limited to several scaffolds, including pyridopyrimidine, azastilbenes, 4-aminoquinolines, aminopyrimidines and pyrrolo[2,3-b]pyridin-2-amine (Fig. 6c)[36]. The lack of potent and selective PKMYT1 inhibitor with new scaffolds has hindered further research. To address this challenge, a virtual screening with KinomeMETA combined with molecular docking was performed to discover new PKMYT1 inhibitor scaffolds. From HTS Compound collection of Life Chemical Screening Library, which contains over 525,000 drug-like compound, 50 candidates were selected and purchased for further experimental evaluation (see method; details of these compounds are shown in Supplementary Table 6). Nine compounds showed inhibition rate >60% in the initial screening performed at 20 μM inhibitor concentration (Fig. 6a). The IC_{50} values were determined for these hits using the FP binding assay, and the potent compounds with inhibitory activity in the low-micromolar range were confirmed (Fig. 6b and Supplementary Fig. 8). Despite the difficulty of inhibiting PKMYT1, as evidenced by the hit rate of 4.17% reported by Davis et al.[33] and 1.25% (10/800) reported by Platzer et al.[35] from known kinase inhibitor libraries, KinomeMETA can distinctly enrich PKMYT1 inhibitors from a large-scale compound library with a high hit rate of 18.00% (9/50), demonstrating its effectiveness for virtual screening.

As shown in Fig. 6c, the spatial projection of newly identified PKMYT1 inhibitors is far from that of known PKMYT1 inhibitors and FDA approved kinase-targeted drugs. This demonstrated that KinomeMETA can identify new PKMYT1 inhibitors with structural novelty, providing different scaffolds such as xanthine (compound 27, 8, and 7), pyrazolo[3,4-d][1,2,4]triazolo[4,3-a]pyrimidin-5-one (compound 26), 1,2,4-oxadiazole (compound 21). These scaffolds are not present in any known PKMYT1 inhibitors and therefore are not used in the training of PKMYT1's model. However, KinomeMETA can still identify these scaffolds since some of them have been identified active for other kinases and trained in the meta-learner. For example, xanthine and its derivatives have been revealed as potential apoptotic antitumor agents that inhibit EGFR, KDR and BRAF[39, 40, 41]. KinomeMETA has incorporated a methylxanthines derivative in the meta-training process on KDR task. Similarly, 1,2,4-Oxadiazole derivatives have been reported to target EGFR and c-Met degradation in TKI resistant NSCLC[42]. In contrast, to the best of our knowledge, pyrazolo[3,4-d][1,2,4]triazolo[4,3-a]pyrimidin-5-one has not been included in any previously approved drugs or known kinase inhibitors. This new scaffold can be referred to as "settler" that contributes to important advancements for new therapies[43].

In summary, the identification of PKMYT1 inhibitors with new scaffolds highlights the KinomeMETA's effectiveness in large-scale virtual screening scenarios. KinomeMETA significantly improves the hit rate in experimental screens for challenging-to-inhibit kinases with limited available inhibitors. Additionally, KinomeMETA's strong generalization ability, which results from its fitting to diverse chemical spaces during meta-training process, facilitates innovation in small molecule drugs by enabling the discovery of structurally novel compounds. This potential for target-specific therapies holds promise for the development of novel and effective treatments.

Retrospective analysis of the inhibitors targeting understudied FGFR mutants.

In the treatment of various types of tumors, fibroblast growth factor receptors (FGFRs) inhibitors have been successfully used [44]. However, gain-of-function mutations in FGFRs can lead to drug resistance, which requires the development of alternative treatment strategies. Identifying new agents that target the gatekeeper and other high incidence resistant mutant of FGFRs could provide therapeutic promise for a subclass of patients of lung cancers, gastric cancer, breast

cancers, etc.[45, 46].

We conducted a retrospective analysis to assess the effectiveness of KinomeMETA in identifying effective and selective inhibitors for FGFR drug-resistant mutants. In our previous study, we obtained a high-potency lead compound 1 as a multi-target FGFRs inhibitor (compound 15[47]) that acts as a multi-target inhibitor of FGFRs. We subsequently synthesized and evaluated a series of derivatives of compound 15[48, 49]. Among these compounds, we identified compound 2e as a highly selective inhibitor for the drug-resistant mutant FGFR2-N549H (Fig. 7a)[49]. Here, we utilized KinomeMETA to predict the kinome spectrum of compound 15 and compound 2e, aiming to evaluate its ability to profile the kinome-wide potency and selectivity of these compounds.

There is limited knowledge about selective inhibitors for some understudied FGFR mutants, such as FGFR1-V561M, FGFR2-V564F, FGFR2-N549H, and FGFR3-V555M. These mutants pose a few-shot learning challenge for KinomeMETA. To address this, we fine-tuned the kinase-specific models according to newly added data. The base-learners for FGFR1-V561M, FGFR2-N549H and FGFR3-V555M were expanded through fast adaption to recently reported compounds (Fig. 7b)[50, 51, 52, 53, 54, 55, 56]. Compared to the moderate performance of the original models of FGFR1-V561M and FGFR2-N549H, the performance of these finetuned models improved, while the performance of FGFR3-V555M remained consistently high (Fig. 7c). Further details regarding the data and model performance of the FGFRs are shown in Supplementary Table 4. Using these fine-tuned models, we conducted kinome profiling to determine the inhibitory probabilities of these compounds against predictable human kinases, and identified compound 2e as a high-selective inhibitor of drug-resistant mutant FGFR2-N549H.

The predictions generated by KinomeMETA agree well with the experimental results obtained from Kinomescan profiling by Eurofins Discovery. The experimental profiling against a panel of 412 kinases at 1 μM concentration indicates that compound 2e could selectively inhibit FGFR2-N549H mutant with an IC_{50} values of 16 nM, and has no substantial inhibitory effect against 95.7% (397/415) tested kinases. For the 331 predictable kinases in the Kinomescan panel, the auROC between experimental and predicted profile of KinomeMETA is up to 0.84 (Fig. 7d). Specifically, for FGFR mutants, KinomeMETA correctly predicted that the compound 2e is active toward FGFR2-N579H, while inactive toward FGFR1-V561M, FGFR2-V564F, and FGFR3-V555M (Fig. 7f). All experimental and predicted results are shown in Supplementary

Table 7.

Moreover, KinomeMETA's high-precision kinome-wide profiling capabilities render it a valuable tool for evaluating selectivity. We calculated the standard scores[3] (see Method) of both the lead compound 15 and the optimized compound 2e. Fig. 7g compared the standard scores obtained from the experimental and predicted profiles for these compounds. These profiles showed consistent trends, indicating the reliability and accuracy of KinomeMETA in assessing selectivity.

To comprehensively assess of the sensitivities of kinase inhibitors, we used KinomeMETA to predict the activity profiles and selectivity scores of 243 kinase inhibitors that are either approved for clinical use or in clinical trials. The obtained results agreed well with the selectivity scores determined by a chemical proteomic approach[57] (Fig. 7e), showing a significant rank correlation (Spearman correlation = 0.752) and similar distribution. The distribution also revealed that compound 2e possesses higher selectivity than most known kinase inhibitors, whereas compound 15 exhibits moderate selectivity. This highlights the potential of KinomeMETA to prioritize inhibitors based on their kinome-wide selectivity.

In conclusion, the experiment confirmed the exceptional predictive performance of KinomeMETA. It may serve as a valuable tool for accurately profiling kinase inhibitors and assessing their selectivity. Moreover, it can effectively address low-data scenarios, such as drug-resistant kinase mutations, due to its ability to incorporate newly added activity compounds.

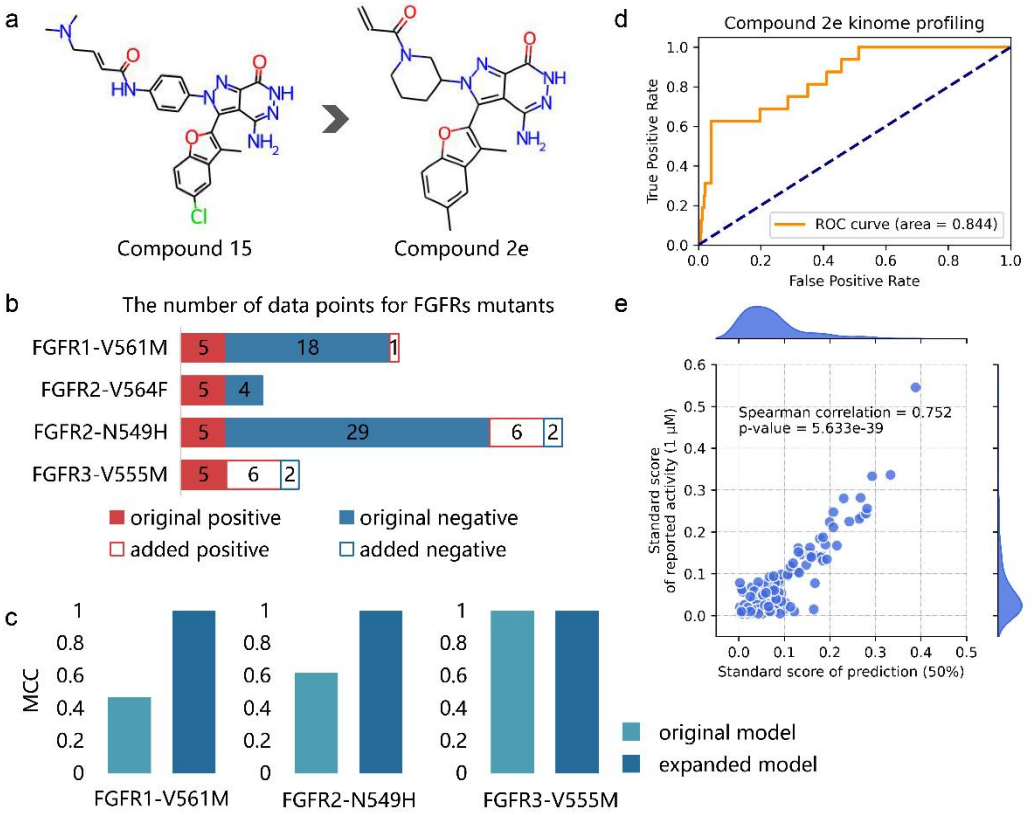

f

kinase	compound 2e	
	IC_{50} (nM)	Predicted probability
FGFR1 V561M	>5000	0.02
FGFR2 N549H	**16**	**0.96**
FGFR2 V564F	2857	0.44
FGFR3 V555M	1999	< 0.001

g

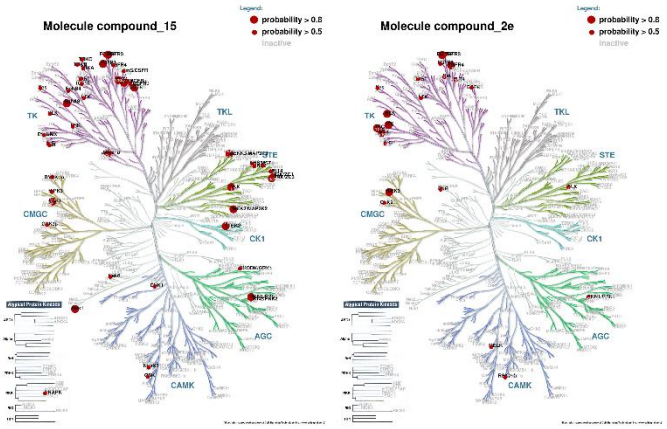

standard score	compound 15	compound 2e
Experimental	0.15 (61 / 405)	**0.04 (18 / 415)**
Predicted	0.18 (95 / 524)	**0.08 (43 / 524)**

Fig. 7 | The retrospective analysis of the inhibitors targeting understudied FGFR mutants. a, Chemical structures of compound 15 and 2e. **b,** Distribution of data points in the base-learners for FGFR1-V561M, FGFR1-V564F, FGFR2-N549H, and FGFR3-V555M. The red solid bars indicate the original number of positive compounds, while the blue solid bars represent the original number of negative compounds. Similarly, the red hollow bars indicate the number of positive compounds added, while the blue hollow bars represent the number of negative compounds added.

c, Model performance measured by MCC for the original and expanded base-learners for FGFR1-V561M, FGFR2-N549H, and FGFR3-V555M. **d,** Model performance measured by ROC curve of compound 2e against 331 predictable kinases screened in the Kinomescan panel. **e,** Distribution of standard scores for 243 kinase inhibitors calculated from KinomeMETA's predicted profile (x-axis) and reported experimental profile (y-axis). **f,** Inhibitory activities and predicted active probability of compound 2e against FGFR mutants. **g,** Phylogenetic tree depicting predicted profiles for compound 15 (left) and compound 2e (right). The table presents standard scores obtained from the experimental and predicted profiles for these compounds.

Discussion

Kinases represent a crucial family of therapeutic targets, especially in cancer treatment. However, the efficacy of kinase inhibitors is limited by drug resistance resulting from mutations and hindered by adverse reactions due to off-target effects. Conventional experimental methods are time-consuming, expensive, and unsuitable for high-throughput screening. Existing computational models have limitations in predicting new diverse kinases or adapting to new kinase tasks with limited data. To address these challenges, we propose KinomeMETA, a general framework for predicting kinome-wide inhibitory activity profile.

KinomeMETA is a powerful tool that integrates meta-learning and GNN with task clustering. This integration enables KinomeMETA to exhibit strong generalization capabilities and rapid adaptability. It consistently outperforms baseline models and other previously reported models across various tasks, including mutated and understudied kinases. Its superior performance may enhance the efficiency of drug screening. For understudied kinases, the identification of structurally novel active compounds can contribute to a better understanding of these kinases. PKMYT1 is a challenging kinase with a low screening hit rate and limited numbers of active compounds. By combining KinomeMETA and molecular docking, we significantly enhanced the hit rate for PKMYT1 (18.00% vs 4.17%), identified new compounds with scaffolds that differ from known active compounds, and greatly reduced the experimental cost (only 50 compounds were tested). On the other hand, KinomeMETA's accurate prediction ability in kinome-wide profiling enables the screening of selective drugs. The selectivity of kinase inhibitors is crucial for their efficacy and safety. FGFR is an important therapeutic target in various cancers, whose

mutations may lead to drug resistance. The retrospective analysis demonstrated that KinomeMETA is capable of identifying compound 2e as a highly selective inhibitor for FGFR2-N549H, surpassing the selectivity of the lead compound 15. This highlights the effectiveness of KinomeMETA in identifying effective and selective inhibitors for FGFR drug-resistant mutants. Adding newly reported data has significantly improved the performance of FGFR mutation task-specific models with limited samples. This feature allows KinomeMETA to quickly adapt to new kinase tasks by learning from a small amount of added data. As a result, KinomeMETA can be further expanded, overcoming the limitations of conventional models that can only predict within a narrow range of kinases or low generalization ability to new kinases.

Although KinomeMETA shows good performance and potential in predicting kinase inhibitory activity, there are still some aspects that can be improved. Firstly, the performance of KinomeMETA is still limited by the quality and quantity of available data, especially for new kinases that differ greatly from those well studied. Therefore, collecting more experimental data to cover a wider range of the kinome will be a direction for further improvement. Secondly, the prediction ability of KinomeMETA may be affected by the diversity and feature representation of compounds. In addition to collecting more data, improving the method of molecular representation is a feasible option. Incorporating 3D information in the molecular representation of KinomeMETA is a promising direction, considering the successful application of these strategies in predicting molecular properties[58]. Additionally, characterizing molecules by phenotypic profiles, such as gene-expression profiles and Cell Painting images, may enable models to capture the connections between biological features of compounds, mitigating the constraints imposed by chemical structural similarity[59].

Overall, KinomeMETA is a valuable tool for rational design of multi-targeted selective kinase inhibitors. It not only helps us quickly identify novel hit compounds through large-scale virtual screening, but also contributes to the design of more effective and safer kinase inhibitor through kinome-wide activity profiling. Its scalability and rapid adaptation for new kinases make it well-suited for exploring so far understudied kinases, which may offer new possibilities for treating more diseases and addressing unmet clinical needs. We envisage that KinomeMETA will become an important component in the future kinase drug discovery and development.

Method

Meta-learning Algorithms

Reptile[27] is a task-agnostic meta-learning algorithm that mathematically similar to first-order MAML[60] (Model-Agnostic Meta-Learning). It takes less computation than MAML by performing standard form stochastic gradient descent (SGD) on each task in a standard form, instead of expanding the calculation graph or calculating any second derivative.

Randomly sampling n tasks in a batch, Reptile algorithm performs SGD on the mixture of all these tasks to update initial parameter vector ϕ each iteration by

$$\phi \leftarrow \phi + \beta \frac{1}{n} \sum_{i=1}^{n} (\widetilde{\phi}_i - \phi)$$

where $\widetilde{\phi}_i = U_{T_i}^{k}(\phi)$ which is the updated parameters on the i^{th} task. Intuitively, for each task, there are parameters that are optimal. Taking several tasks, Reptile tries to get the initialization parameters for which the distance to the optimal parameters for each task is minimal. Then, based on the initialization that broadly suitable for many tasks, a small number of gradient updates will lead to fast learning on a new similar task. Hence, Reptile-based KinomeMETA first produce an agent (model), i.e., meta-learner, that has good average performance on any kinase task. Then, the meta-learner can be fine-tuned slightly (fast adaptation) with the least samples (compounds with bioactivity data) that are task-specific to reach the optimum base-learner for any new kinase task.

Molecular representation algorithm

In this study, a graph attention neural network-based molecular representation algorithm called Attentive-FP[28] was embedded into Reptile. Attentive-FP is a molecular representation model, which directly takes the structural feature of small molecules as input, and defines molecules as graphs composed of nodes (atoms) and edges (bonds). The molecular graph of drugs is regarded as the structural data of the graph, which is more flexible than the predefined molecular descriptors and fingerprints. In particular, Attentive-FP introduces attention mechanisms at both local and global levels, assigning different weights to different parts of the input, so that the model can extract key parts of the input information.

Hierarchical clustering for tasks based on protein embedding

Task heterogeneity is a critical challenge in meta-learning, which is limited to settings where the current task is closely related to previous ones[61]. However, distribution heterogeneity on sequences and structures of the protein kinases[62], means that in practical transfer learning scenarios the new kinase task might not be tightly linked to previous kinases learned in the meta-learner. In addition, given the imbalanced kinase groups, overfitting to a dominant group such as TK will impair global generalization.

Hence, to consider the task heterogeneity in the procedure of meta-training to promote generalization, tasks were hierarchically clustered based on its protein embedding. Protein embedding was generated from ESM-1b. ESM-1b is an advanced deep protein language modeling that condense protein sequence to learn chemical and biological concepts including structure, function, binding, etc., which could address the shortcomings in commonly used Phylogenetic trees[63, 64]. Then, the hierarchical clustering average linkage algorithm was used to cluster the protein embedding. Average linkage represents a way to measure the dissimilarity between groups of samples, in which dissimilarity between groups R and S is the average dissimilarity between each point in one group and each point in another group:

$$D(R,S) = \underset{i \in R, j \in S}{\text{avg}} d_{ij}$$

Accordingly, all 661 kinases (including mutations) were divided into 12 groups, including a group for all outlier kinases. Supplementary Fig. 2a illustrates the distribution of kinase clusters, while Supplementary Fig. 2b displays the distribution of the training, validation, and test kinases sampled from these clusters.

Metrics

For model quality assessment, the auROC (area under the ROC curve), Recall, Precision, F1-score, MCC (Matthews correlation coefficient) and BACC (balanced accuracy) were evaluated (Table 1). The MCC is the metric we mainly discussed in this work, as is a more reliable statistical rate which produces a high score only if the prediction obtained good results in all of the four confusion matrix categories. It can produce a more informative and truthful score in evaluating label-imbalanced binary classifications than auROC, accuracy and F1-score[65].

Table 1. Description of the Evaluation Metrics

evaluation metric	equation
Recall	TP/ (TP + FN)
Precision	TP/ (TP + FP)
F1-score	$2\times \frac{Precision \times Recall}{Precision + Recall}$
MCC	$\frac{TP\times TN - FP\times FN}{\sqrt{(TP+FP)(TP+FN)(TN+FP)(TN+FN)}}$
BACC	$(\frac{TP}{TP+FN} + \frac{TN}{FP+TN})/2$

*TP is the number of correctly predicted actives (true positives). TN is the number of correctly predicted inactive (true negatives). FP is the number of incorrectly identified actives (false positives), and FN is the number of incorrectly identified inactive (false negatives).

Standard score

The standard score is computed by dividing the number of kinase hits above or below a threshold value by the total number of kinases tested. In the case of the predicted profile, the standard score is calculated by dividing the number of kinases predicted as positive (probability > 0.5) by the total number of predictable human kinases (524). For the experimental profile of compound 15 and 2e, the standard scores are determined by dividing the number of kinase hits above a threshold of 50% inhibition at 1 μM by the total number of kinases tested. In Fig. 7e, which displays data for 243 kinase inhibitors, the standard scores are calculated by dividing the number of kinase hits above a threshold of 1000 nM (IC_{50} determined by a chemical proteomic approach) by the total number of kinases tested.

Virtual screening and experimental evaluation for PKMYT1

First, the kinase-specific base-learners of PKMYT1 were applied to score the compounds from the HTS Compound collection of Life Chemical Screening Library, which contains over 525,000 drug-like compounds. Second, all other kinase-specific base-learners were applied to predicted the kinome spectrum to calculate selectivity scores for these compounds. Third, compounds with PKMYT1 probability > 0.5 and selectivity score < 0.25 were selected for further molecular docking to the crystal structure of PKMYT1 (PDB accession code: 8D6E) via the

Maestro module of Schrödinger software package. Finally, after filtered pan assay interference compounds (PAINS) and clustered these molecules automatically based on their extended connectivity fingerprints (ECFP), a total of 50 candidates were purchased for further experimental evaluation. The initial screening was performed at 20 μM inhibitor concentration, with RP-6306 (1 μM) used as inhibitory control (100% effect, measured as displacement) and 1% DMSO as vehicle control (0% displacement). The IC_{50} values for nine compounds with a tracer displacement >60% were determined for confirmed hits using the FP binding assay.

Abbreviations

AI: Artificial Intelligence; PKMYT1: Membrane-associated tyrosine- and threonine-specific cdc2-inhibitory kinase; FGFR: Fibroblast growth factor receptor; KIT: KIT Proto-Oncogene, Receptor Tyrosine Kinase; ABL1: ABL proto-oncogene 1, non-receptor tyrosine kinase; EGFR: Epidermal growth factor receptor; ALK: Anaplastic lymphoma kinase; MET: its encoding protein called c-Met, cellular-mesenchymal to epithelial transition factor; FLT3: Fms-like Receptor Tyrosine Kinase 3; RET: Rearranged during transfection receptor tyrosine kinase; CDK1: cyclin-dependent kinase 1; CCNE1: cyclin E1; Wee1: WEE1 G2 checkpoint kinase; KDR: Kinase insert domain receptor; BRAF:B-Raf Proto-Oncogene, Serine/Threonine Kinase; NB: Naive Bayes; RF: Random Forest; SVM: Support Vector Machine; DNN: Deep Neural Network; ST: Single-Task; MT: Multi-Task; ECFP: extended connectivity fingerprint; DMSO: Dimethyl Sulfoxide; ML: Machine Learning; DL: Deep Learning; GNN: Graph Neural Network; GCN: Graph Convolution Network; AI: Artificial Intelligence; MAML: Model-Agnostic Meta-Learning; SGD: Stochastic gradient descent; UMAP: Uniform manifold approximation and projection; DKKB: Dark Kinase Knowledgebase; PKIS: protein kinase inhibitor set; FDA: Food and Drug Administration; PDB: Protein Data Bank; IC_{50}: half maximal inhibitory concentration; K_i: inhibitor constant; EC_{50}: half maximal effective concentration; K_d: dissociation constant; %Inh: percentage inhibition rate; pK_i: $-\log_{10}K_i$; pK_d: $-\log_{10}K_d$; pIC_{50}: $-\log_{10}IC_{50}$; pEC_{50}: $-\log_{10}EC_{50}$; TK: Tyrosine kinase; TKL: Tyrosine Kinase-Like kinase; TKI: Tyrosine Kinase Inhibitor; NSCLC: Non-Small Cell Lung Cancer; HTS: High Throughput Screening; PAINS: pan assay interference compounds; logP: $\log_{10}$ (Partition Coefficient); μM: Micrometre; nM: Nanometre; FP binding

assay: Fluorescence Polarization binding assay; auROC: area under the ROC curve; MCC: Matthews correlation coefficient; BACC: balanced accuracy.

Declarations

Code availability

The source codes and related data of KinomeMETA are available at: https://github.com/tunequ/KinomeMeta.

Competing interests

The authors declare no competing interests.

Funding

This work was supported by National Natural Science Foundation of China (T2225002 and 82273855 to M.Y.Z., 82204278 to X.T.L.), Lingang Laboratory (LG202102-01-02 to M.Y.Z.), National Key Research and Development Program of China (2022YFC3400504 to M.Y.Z.), SIMM-SHUTCM Traditional Chinese Medicine Innovation Joint Research Program (E2G805H to M.Y.Z.), China Postdoctoral Science Foundation (2022M720153 to X.T.L.), and Shanghai Municipal Science and Technology Major Project.

Authors' contributions

M.Y.Z. and X.T.L. conceived the project. Q.R. and N.Q. implemented the KinomeMETA model and conducted computational analysis. J.J.S, J.L., L.N., X.C.T., Z.M.Z, X.T.K., Y.M.W and Y.T.W. helped to collect and analyze the data. Q.R., X.T.L, N.Q. and M.Y.Z. wrote the paper. All authors discussed the results and commented on the manuscript.

Authors' details

[1] Drug Discovery and Design Center, State Key Laboratory of Drug Research, Shanghai Institute of Materia Medica, Chinese Academy of Sciences, 555 Zuchongzhi Road, Shanghai 201203,

China

[2] University of Chinese Academy of Sciences, No.19A Yuquan Road, Beijing 100049, China

[3] Nanjing University of Chinese Medicine, 138 Xianlin Road, Nanjing 210023, China

[4] College of Pharmaceutical Sciences, Zhejiang University, Hangzhou 310058, China

[5] School of Pharmaceutical Science and Technology, Hangzhou Institute for Advanced Study, UCAS, Hangzhou 330106, China

[6] Lingang Laboratory, Shanghai 200031, China

[#] Qun Ren and Ning Qu have contributed equally to this work

[*] Correspondence: myzheng@simm.ac.cn; lixutong@simm.ac.cn

1. Cohen P. Protein kinases — the major drug targets of the twenty-first century? *Nature Reviews Drug Discovery* **1**, 309-315 (2002).

2. Noble MEM, Endicott JA, Johnson LN. Protein Kinase Inhibitors: Insights into Drug Design from Structure. *Science* **303**, 1800-1805 (2004).

3. Karaman MW*, et al.* A quantitative analysis of kinase inhibitor selectivity. *Nature Biotechnology* **26**, 127-132 (2008).

4. Gentile C, Martorana A, Lauria A, Bonsignore R. Kinase Inhibitors in Multitargeted Cancer Therapy. *Current medicinal chemistry* **24**, 1671-1686 (2017).

5. Samarasinghe KTG, Crews CM. Targeted protein degradation: A promise for undruggable proteins. *Cell chemical biology* **28**, 934-951 (2021).

6. Reinecke M, Heinzlmeir S, Wilhelm M, Médard G, Klaeger S, Kuster B. Kinobeads: A Chemical Proteomic Approach for Kinase Inhibitor Selectivity Profiling and Target Discovery. In: *Target Discovery and Validation*) (2019).

7. Niijima S, Shiraishi A, Okuno Y. Dissecting Kinase Profiling Data to Predict Activity and Understand Cross-Reactivity of Kinase Inhibitors. *Journal of*

Chemical Information and Modeling **52**, 901-912 (2012).

8. Merget B, Turk S, Eid S, Rippmann F, Fulle S. Profiling Prediction of Kinase Inhibitors: Toward the Virtual Assay. *Journal of Medicinal Chemistry* **60**, 474-485 (2017).

9. Lapins M, Wikberg JES. Kinome-wide interaction modelling using alignment-based and alignment-independent approaches for kinase description and linear and non-linear data analysis techniques. *BMC Bioinformatics* **11**, 339 (2010).

10. Yabuuchi H*, et al.* Analysis of multiple compound–protein interactions reveals novel bioactive molecules. *Molecular Systems Biology* **7**, 472 (2011).

11. Schürer SC, Muskal SM. Kinome-wide Activity Modeling from Diverse Public High-Quality Data Sets. *Journal of Chemical Information and Modeling* **53**, 27-38 (2013).

12. Manallack DT*, et al.* Selecting Screening Candidates for Kinase and G Protein-Coupled Receptor Targets Using Neural Networks. *Journal of Chemical Information and Computer Sciences* **42**, 1256-1262 (2002).

13. Rodríguez-Pérez R, Bajorath J. Multitask Machine Learning for Classifying Highly and Weakly Potent Kinase Inhibitors. *ACS Omega* **4**, 4367-4375 (2019).

14. Li X*, et al.* Deep Learning Enhancing Kinome-Wide Polypharmacology Profiling: Model Construction and Experiment Validation. *Journal of Medicinal Chemistry* **63**, 8723-8737 (2020).

15. Bao L*, et al.* Kinome-wide polypharmacology profiling of small molecules by multi-task graph isomorphism network approach. *Acta Pharmaceutica Sinica B* **13**, 54-67 (2023).

16. Shen C, Luo J, Ouyang W, Ding P, Chen X. IDDkin: network-based influence deep diffusion model for enhancing prediction of kinase inhibitors. *Bioinformatics* **36**, 5481-5491 (2020).

17. Wang J, Zheng S, Chen J, Yang Y. Meta Learning for Low-Resource Molecular Optimization. *Journal of Chemical Information and Modeling* **61**, 1627-1636 (2021).

18. Ma J*, et al.* Few-shot learning creates predictive models of drug response that translate from high-throughput screens to individual patients. *Nature Cancer* **2**, 233-244 (2021).

19. Cai T*, et al.* End-to-end sequence-structure-function meta-learning predicts genome-wide chemical-protein interactions for dark proteins. *PLOS Computational Biology* **19**, e1010851 (2023).

20. Gao Y*, et al.* Pan-Peptide Meta Learning for T-cell receptor–antigen binding recognition. *Nature Machine Intelligence* **5**, 236-249 (2023).

21. Hospedales TM, Antoniou A, Micaelli P, Storkey AJJIToPA, Intelligence M. Meta-Learning in Neural Networks: A Survey. **44**, 5149-5169 (2020).

22. Saikin SK, Kreisbeck C, Sheberla D, Becker JS, A AG. Closed-loop discovery platform integration is needed for artificial intelligence to make an impact in drug discovery. *Expert opinion on drug discovery* **14**, 1-4 (2019).

23. Mendez D*, et al.* ChEMBL: towards direct deposition of bioassay data. *Nucleic Acids Research* **47**, D930-D940 (2019).

24. Kim S*, et al.* PubChem in 2021: new data content and improved web interfaces. *Nucleic Acids Research* **49**, D1388-D1395 (2021).

25. Berginski ME, Moret N, Liu C, Goldfarb D, Sorger Peter K, Gomez SM. The Dark Kinase Knowledgebase: an online compendium of knowledge and experimental results of understudied kinases. *Nucleic Acids Research* **49**, D529-D535 (2021).

26. Imrie F, Bradley AR, Deane CM. Generating property-matched decoy molecules using deep learning. *Bioinformatics* **37**, 2134-2141 (2021).

27. Nichol A, Achiam J, Schulman JJA. On First-Order Meta-Learning Algorithms. *ArXiv* **abs/1803.02999**, (2018).

28. Xiong Z*, et al.* Pushing the Boundaries of Molecular Representation for Drug Discovery with the Graph Attention Mechanism. *Journal of Medicinal Chemistry* **63**, 8749-8760 (2020).

29. Kumar A, Daumé H. Learning task grouping and overlap in multi-task learning. In: *Proceedings of the 29th International Coference on International Conference on Machine Learning*). Omnipress (2012).

30. Goyal A, Bengio YJPotRSA. Inductive biases for deep learning of higher-level cognition. **478**, (2020).

31. Naga D, Muster W, Musvasva E, Ecker GF. Off-targetP ML: an open source

machine learning framework for off-target panel safety assessment of small molecules. *Journal of Cheminformatics* **14**, 27 (2022).

32. Gallo D*, et al.* CCNE1 amplification is synthetic lethal with PKMYT1 kinase inhibition. *Nature* **604**, 749-756 (2022).

33. Davis MI*, et al.* Comprehensive analysis of kinase inhibitor selectivity. *Nature Biotechnology* **29**, 1046-1051 (2011).

34. Rohe A*, et al.* Evaluation of potential Myt1 kinase inhibitors by TR-FRET based binding assay. *European Journal of Medicinal Chemistry* **61**, 41-48 (2013).

35. Platzer C, Najjar A, Rohe A, Erdmann F, Sippl W, Schmidt M. Identification of PKMYT1 inhibitors by screening the GSK published protein kinase inhibitor set I and II. *Bioorganic & Medicinal Chemistry* **26**, 4014-4024 (2018).

36. Najjar A*, et al.* Computer-aided design, synthesis and biological characterization of novel inhibitors for PKMYT1. *European Journal of Medicinal Chemistry* **161**, 479-492 (2019).

37. Chakravarty S*, et al.* Substituted pyrazolo [3, 4-d] pyrimidines as Wee1 inhibitors Patent US11332473B2 (2022).

38. Szychowski J*, et al.* Discovery of an Orally Bioavailable and Selective PKMYT1 Inhibitor, RP-6306. *Journal of Medicinal Chemistry* **65**, 10251-10284 (2022).

39. Luo C, Xie P, Marmorstein R. Identification of BRAF Inhibitors through In Silico Screening. *Journal of Medicinal Chemistry* **51**, 6121-6127 (2008).

40. Abuo-Rahma GE-DAA, Abdel-Aziz M, Beshr EAM, Ali TFS. 1,2,4-Triazole/oxime hybrids as new strategy for nitric oxide donors: Synthesis, anti-inflammatory, ulceroginicity and antiproliferative activities. *European Journal of Medicinal Chemistry* **71**, 185-198 (2014).

41. Hisham M, Youssif BGM, Osman EEA, Hayallah AM, Abdel-Aziz M. Synthesis and biological evaluation of novel xanthine derivatives as potential apoptotic antitumor agents. *European Journal of Medicinal Chemistry* **176**, 117-128 (2019).

42. Dokla EME, Fang C-S, Abouzid KAM, Chen CS. 1,2,4-Oxadiazole derivatives targeting EGFR and c-Met degradation in TKI resistant NSCLC. *European Journal of Medicinal Chemistry* **182**, 111607 (2019).

43. Wills TJ, Lipkus AH. Structural Approach to Assessing the Innovativeness of

New Drugs Finds Accelerating Rate of Innovation. *ACS Medicinal Chemistry Letters* **11**, 2114-2119 (2020).

44. Dai S, Zhou Z, Chen Z, Xu G, Chen Y. Fibroblast Growth Factor Receptors (FGFRs): Structures and Small Molecule Inhibitors. *Cells* **8**, (2019).

45. Liang G, Chen G, Wei X, Zhao Y, Li X. Small molecule inhibition of fibroblast growth factor receptors in cancer. *Cytokine & Growth Factor Reviews* **24**, 467-475 (2013).

46. Touat M, Ileana E, Postel-Vinay S, André F, Soria JC. Targeting FGFR Signaling in Cancer. *Clinical cancer research : an official journal of the American Association for Cancer Research* **21**, 2684-2694 (2015).

47. Wang Y*, et al.* Discovery and Development of a Series of Pyrazolo[3,4-d]pyridazinone Compounds as the Novel Covalent Fibroblast Growth Factor Receptor Inhibitors by the Rational Drug Design. *Journal of Medicinal Chemistry* **62**, 7473-7488 (2019).

48. Wu X*, et al.* Design, synthesis and biological evaluation of pyrazolo[3,4-d]pyridazinone derivatives as covalent FGFR inhibitors. *Acta Pharmaceutica Sinica B* **11**, 781-794 (2021).

49. Li C*, et al.* Structural Optimization of Fibroblast Growth Factor Receptor Inhibitors for Treating Solid Tumors. *Journal of Medicinal Chemistry* **66**, 3226-3249 (2023).

50. Yue S*, et al.* FGFR-TKI resistance in cancer: current status and perspectives. *Journal of Hematology & Oncology* **14**, 23 (2021).

51. Shvartsbart A*, et al.* Discovery of Potent and Selective Inhibitors of Wild-Type and Gatekeeper Mutant Fibroblast Growth Factor Receptor (FGFR) 2/3. *Journal of Medicinal Chemistry* **65**, 15433-15442 (2022).

52. Peng X*, et al.* Preclinical evaluation of 3D185, a novel potent inhibitor of FGFR1/2/3 and CSF-1R, in FGFR-dependent and macrophage-dominant cancer models. *Journal of Experimental & Clinical Cancer Research* **38**, 372 (2019).

53. Xie W*, et al.* Discovery of 2-Amino-7-sulfonyl-7H-pyrrolo[2,3-d]pyrimidine Derivatives as Potent Reversible FGFR Inhibitors with Gatekeeper Mutation Tolerance: Design, Synthesis, and Biological Evaluation. *Journal of Medicinal Chemistry* **65**, 16570-16588 (2022).

54. Shao M*, et al.* Design, Synthesis, and Biological Evaluation of Aminoindazole Derivatives as Highly Selective Covalent Inhibitors of Wild-Type and Gatekeeper Mutant FGFR4. *Journal of Medicinal Chemistry* **65**, 5113-5133 (2022).

55. Ryu S*, et al.* Identification of Pyridinyltriazine Derivatives as Potent panFGFR Inhibitors against Gatekeeper Mutants for Overcoming Drug Resistance. *Journal of Medicinal Chemistry* **65**, 6017-6038 (2022).

56. Xie Z*, et al.* Discovery of 4,6-pyrimidinediamine derivatives as novel dual EGFR/FGFR inhibitors aimed EGFR/FGFR1-positive NSCLC. *European Journal of Medicinal Chemistry* **187**, 111943 (2020).

57. Klaeger S*, et al.* The target landscape of clinical kinase drugs. *Science* **358**, eaan4368 (2017).

58. Shengchao L, Hanchen W, Weiyang L, Joan L, Hongyu G, Jian T. Pre-training Molecular Graph Representation with 3D Geometry. In: *International Conference on Learning Representations*) (2022).

59. Moshkov N*, et al.* Predicting compound activity from phenotypic profiles and chemical structures. *Nat Commun* **14**, 1967 (2023).

60. Finn C, Abbeel P, Levine S. Model-Agnostic Meta-Learning for Fast Adaptation of Deep Networks. In: *Proceedings of the 34th International Conference on Machine Learning* (eds Doina P, Yee Whye T). PMLR (2017).

61. Day O, Khoshgoftaar TM. A survey on heterogeneous transfer learning. *Journal of Big Data* **4**, 29 (2017).

62. Manning G, Whyte DB, Martinez R, Hunter T, Sudarsanam S. The Protein Kinase Complement of the Human Genome. *Science* **298**, 1912-1934 (2002).

63. Rives A*, et al.* Biological structure and function emerge from scaling unsupervised learning to 250 million protein sequences. *Proceedings of the National Academy of Sciences* **118**, e2016239118 (2021).

64. Paricharak S, Klenka T, Augustin M, Patel UA, Bender A. Are phylogenetic trees suitable for chemogenomics analyses of bioactivity data sets: the importance of shared active compounds and choosing a suitable data embedding method, as exemplified on Kinases. *Journal of Cheminformatics* **5**, 49 (2013).

65. Chicco D, Jurman G. The advantages of the Matthews correlation coefficient (MCC) over F1 score and accuracy in binary classification evaluation. *BMC*

951 *Genomics* **21**, 6 (2020).
952
953
954
955